Modification of Mn_3O_4 Thin Films by Fe Doping: Structural, Morphological and Optical Studies

Priyanka B. Biradar[1]; Vijendra A. Chaudhari[2]

[1]Dayanand Science College, Latur.
[2]Dayanand Science College, Latur.

Publication Date: 2026/08/12

Abstract: The effect of Fe incorporation on the structural, morphological, and optical properties of pure Mn_3O_4 and 5 mol% Fe-doped Mn_3O_4 is investigated. Thin films deposited on glass substrates by the spray pyrolysis technique have been studied. The X-ray diffraction analysis confirmed the formation of a single-phase tetragonal hausmannite Mn_3O_4 structure (JCPDS card No. 24-0734) for both films without any secondary phases that could be detected. Fe doping reduced the average crystallite size from 22.14 to 20.04 nm with an increase in microstrain and dislocation density. The decrease in lattice parameters and unit-cell volume further confirms the incorporation of Fe, leading to modification of the crystal lattice, while the phase composition is still retained. FESEM analysis indicated that the doped film had a better surface morphology and a denser distribution of finer grains than the undoped film. Optical measurements revealed a decreased band gap from 2.61 eV for pure Mn_3O_4 to 2.38 eV after Fe doping, indicating a change in the electronic structure of the material. The change in structure, morphology, and optical properties together suggests that Fe doping is an effective way to tune the properties of Mn_3O_4 thin films. These results pave the way for further investigations of the Fe-doped Mn_3O_4 facility. for applications where surface and electronic properties are critical.

Keywords: *Mn_3O_4, Fe-Doped Manganese Oxide, Spray Pyrolysis, Crystal Structure, Surface Morphology, Optical Properties.*

How to Cite: Priyanka B. Biradar; Vijendra A. Chaudhari (2026) Modification of Mn_3O_4 Thin Films by Fe Doping: Structural, Morphological and Optical Studies. *International Journal of Innovative Science and Research Technology*, 11(8), 210-215. https://doi.org/10.38124/ijisrt/26aug363

I. INTRODUCTION

Metal oxides are a fundamental category of materials in modern research, distinguished by their adaptable optical and electrical properties that facilitate a variety of technological advancements. Manganese oxide has garnered significant scholarly interest due to its classification as a multifunctional metal oxide semiconductor. This classification provides unique electrical and optical properties that are essential for the development of optoelectronic devices, gas detection, and energy storage. [1–4]. Among the diverse manganese oxide phases, this specific phase is especially distinguished by its thermodynamic stability and advantageous physicochemical characteristics. [5]. As a p-type semiconductor, it possesses a tetragonal spinel configuration, wherein the presence of ions at the octahedral B-site results in a notable Jahn-Teller distortion. [6]. This semiconductor is extensively employed in catalytic, battery, and sensor applications owing to its extensive functional adaptability. [7]. Despite its potential, bulk Mn_3O_4often requires optimization to enhance its functional performance, with recent studies highlighting the necessity of cost-effective, low-temperature synthesis techniques like spray pyrolysis for thin-film fabrication[8],[9]. The introduction of transition metal dopants into the spinel lattice acts as a tactical method to adjust charge carrier behavior and expand the band gap for enhanced optoelectronic efficacy. [10]. The choice of Fe as a dopant at a 5% concentration is intended to modify the lattice characteristics and electronic density of states, thus enhancing the carrier mobility of the hausmannite phase. [11,12].

The main aim of this study is to produce high-quality pure and 5% Fe-doped thin films via chemical spray pyrolysis to methodically assess the influence of iron addition on the structural, morphological, and optical characteristics of the hausmannite structure. Additionally, this research aims to clarify the relationship between iron-induced structural changes and the consequent alterations in optical band gap energy, thereby offering a thorough evaluation of the material's appropriateness for sophisticated semiconductor applications. [13,14]. This study aims to create a framework for improving the inherent characteristics of materials via impurity-driven lattice manipulation by meticulously regulating the dopant levels. [10,15]. This systematic approach provides a fundamental understanding of how

ISSN No:-2456-2165 https://doi.org/10.38124/ijisrt/26aug363

localized Fe substitutions influence the stoichiometric stability of the hausmannite phase [16,17]. Furthermore, the investigation aims to correlate these structural adjustments with potential shifts in the optical band gap, thereby providing critical insights into the band structure engineering of doped spinels [18].

The goal of this work is to determine whether Fe-doped Mn3O4 thin films are a viable option for integration into advanced gas sensing systems. In order to detect volatile organic compounds and other hazardous gasses in practical sensing applications, this study will elucidate how different levels of iron doping affect structural, morphological, and optical changes, which in turn affect surface reactivity and charge carrier transport mechanisms. [13,17] This endeavor is particularly pertinent given the reported efficacy of transition metal ion doping in refining the separation efficiency of photo-generated carriers and expanding the photo-response range of manganese-based materials [19]. Moreover, the strategic integration of iron ions offers a controlled pathway to refine the electronic states within the Mn_3O_4 band structure, which is essential for optimizing gas-sensing performance [3].

II. MATERIALS AND METHODS

For the synthesis of 5 mol% Fe-doped Mn_3O_4 thin films, the precursor solution was prepared using the spray pyrolysis method. First, 0.2703 g of $FeCl_3{\cdot}6H_2O$ was dissolved in 10 mL of double-distilled water to create a 0.1 M iron stock solution. By replacing 1.0 mL of the 0.1 M manganese precursor solution with an equivalent amount of the iron precursor solution, the goal doping concentration was reached, resulting in a nominal Fe concentration of 5 mol%. As a result, throughout this investigation, the resultant films are referred to as 5 mol% Fe-doped Mn3O4. The final mixed precursor solution was magnetically stirred at room temperature for 5 minutes and was then used immediately for film deposition. Pure and 5 mol% Fe-doped Mn_3O_4 thin films were deposited on microscope glass slides (25×75×1 mm) as substrates. Before the substrates were washed with Labolene solution to remove deposition, they were first washed with Labolene solution to remove surface contaminants. Then, they were immersed in chromic acid and finally heated for 1 hour. The substrates were cooled to room temperature by natural cooling and then washed extensively with tap water to remove any residual chromic acid. Before being deposited, they were cleaned with double-distilled water, cleaned with acetone, and dried.

The thin films were deposited using a spray pyrolysis system equipped with a stainless-steel pneumatic air-assisted atomizing nozzle. The precursor solution was atomized using compressed air delivered via a pressure regulator and sprayed onto preheated substrates maintained at 400°C. The substrate temperature was monitored using a thermocouple throughout the deposition process. The carrier gas pressure was maintained at 30 psi, while the precursor solution was delivered continuously at a flow rate of 2 mL min^{-1}. The distance between the spray nozzle and the substrate was fixed at 30 cm. For each deposition, 20 mL of precursor solution was sprayed, and three glass substrates were coated simultaneously. After deposition, the films were allowed to cool naturally on the substrate heater to room temperature.

III. RESULTS

The X-ray diffraction (XRD) patterns of pure and 5% Fe-doped Mn_3O_4 thin films are presented in Fig. 1. The diffraction peaks observed at the indexed planes of (112), (200), (103), (211), (004), (220), (105), (312), (321), (224), and (314) are in good agreement with the tetragonal hausmannite Mn_3O_4 phase (JCPDS card No. 24-0734), thereby validating the establishment of the intended crystalline phase. [20,21]. The broadening of these diffraction peaks upon doping indicates a slight decrease in crystallite size, suggesting that the incorporation of iron ions disrupts long-range periodic order within the hausmannite lattice [22,23]. Furthermore, the systematic shift of the reflection toward higher diffraction angles in the doped samples indicates a contraction of the unit cell volume, likely resulting from the substitution of larger cations by smaller ions within the spinel framework [24].

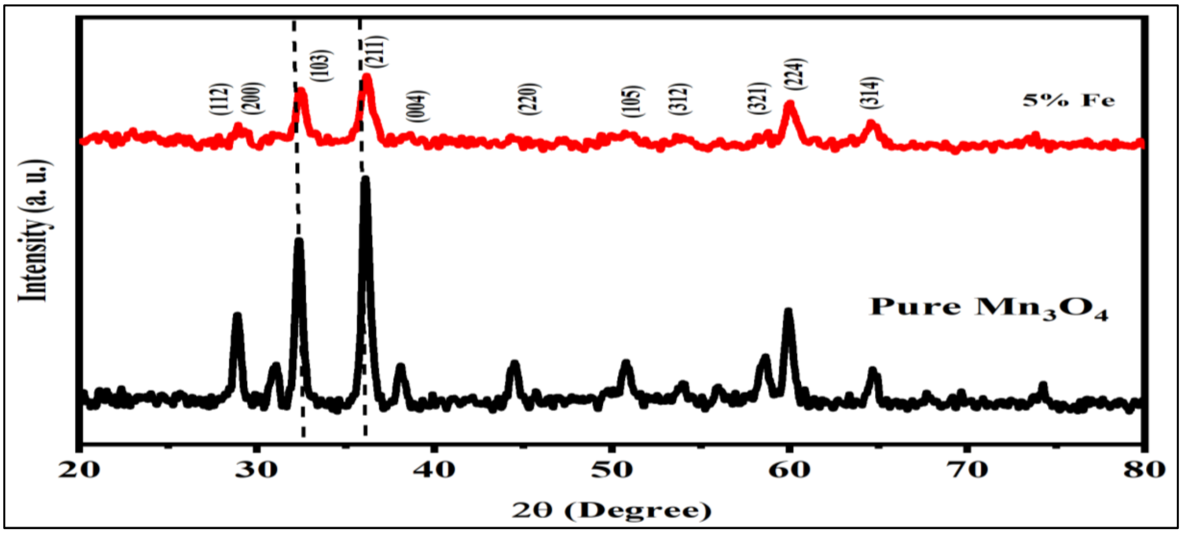

Fig 1 The X-ray Diffraction (XRD) Patterns of Pure and 5% Fe-Doped Mn_3O_4 Thin Films

ISSN No:-2456-2165 https://doi.org/10.38124/ijisrt/26aug363

Table 1 The Structural Parameters Derived from the XRD Data

Sample	D (nm)	Dislocation Density (nm^2)	Strain	d	a=b (Å)	c (Å)	Volume (Å³)	u Parameter	Bond Length (Å)	Distortion Parameter
Pure Mn_3O_4	22.1375	0.0461	0.0051	2.3824	5.7624	9.4521	313.8657	0.3738	3.5340	0.6403
5% Fe	20.0449	0.0629	0.0066	2.3737	5.7492	9.2247	304.9115	0.3794	3.5005	0.6045

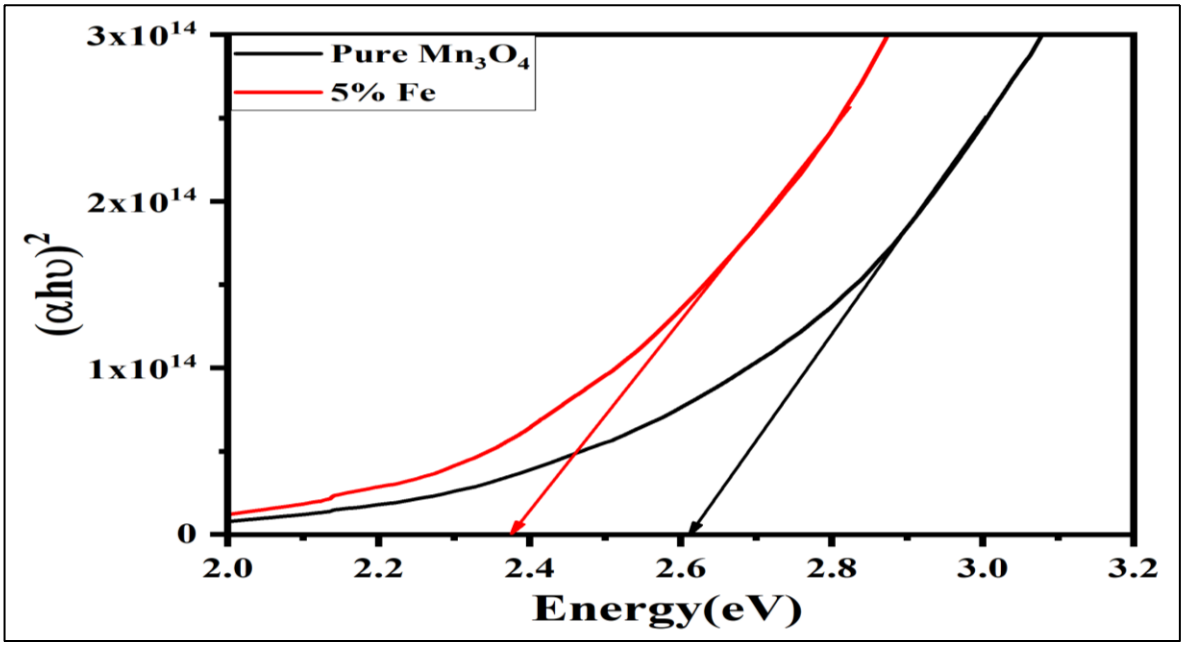

Fig 2 The Optical Band Gap of the Pure and 5% Fe-Doped Mn_3O_4 Thin Films

The optical band gap of the pure and 5% Fe-doped Mn_3O_4 thin films was evaluated using the Tauc relation by plotting $(\alpha h\nu)^2$ as a function of photon energy (hν), as shown in Fig. 2. The band gap energy was obtained by extrapolating the linear portion of each plot to the energy axis. The pure Mn_3O_4 film exhibits a band gap of 2.61 eV, which decreases to 2.38 eV after the incorporation of 5 mol.% Fe.

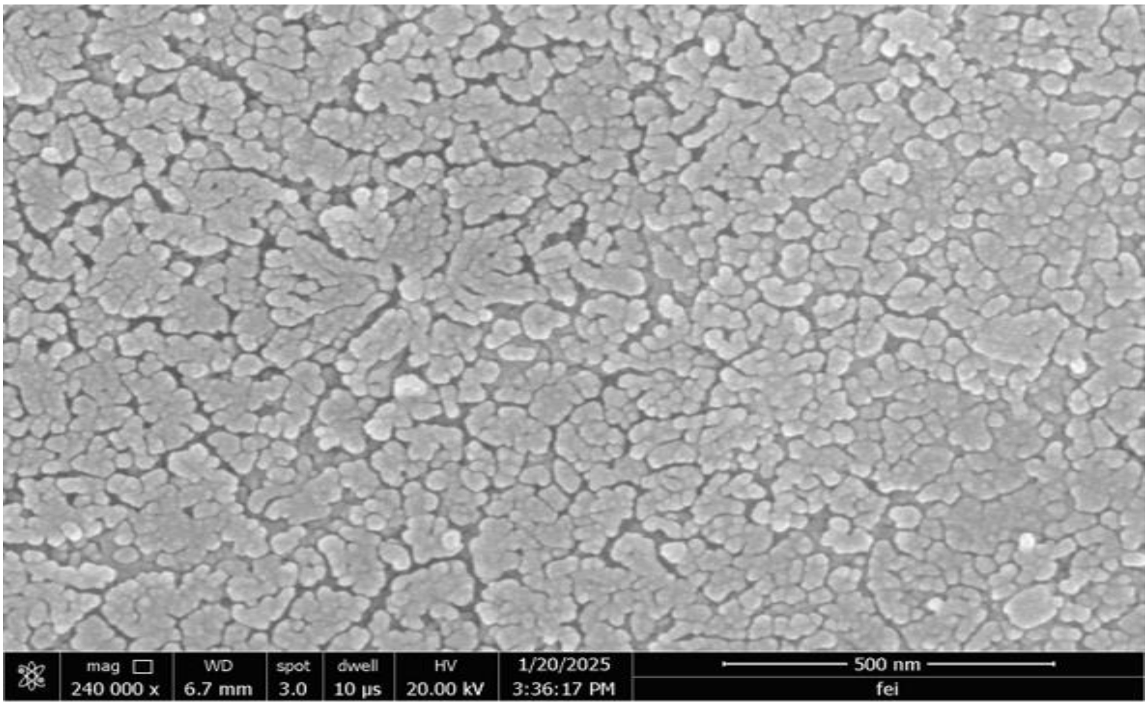

ISSN No:-2456-2165 https://doi.org/10.38124/ijisrt/26aug363

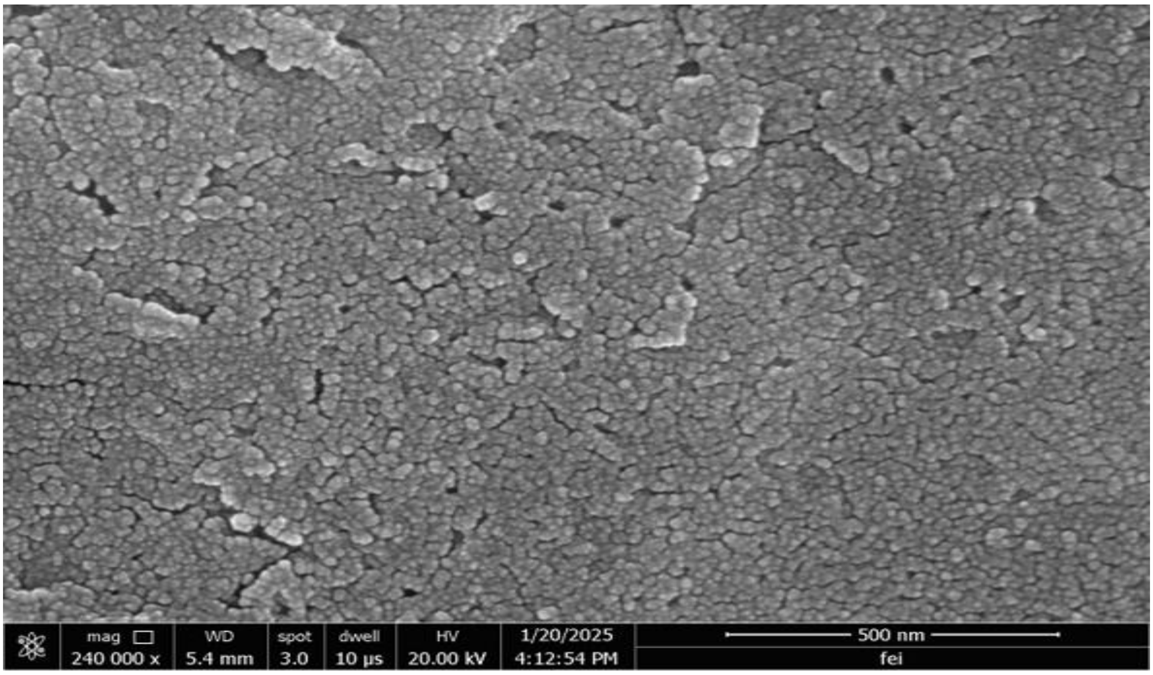

Fig 3 (a–b) Shows the FESEM Micrographs of the Pure and 5 mol% Fe-Doped Mn_3O_4 Thin Films

The surface of the pure Mn_3O_4 film (Fig. 3a) is composed of densely packed grains distributed uniformly over the substrate. There is no indication of large agglomerates or uncovered regions, and the grains are nearly spherical in shape. They form a continuous, compact microstructure. In contrast, the incorporation of 5 mol% Fe results in a significant reduction in particle size, which is characterized by a highly interconnected surface texture and a more porous morphology. The film maintains a continuous and homogeneous surface morphology following the incorporation of 5 mol% Fe (Fig. 3b); however, the grains are more closely packed and finer than those of the pure Mn_3O_4 film.

IV. DISCUSSION

The average crystallite size (D) decreases from 22.14 nm for the pure film to 20.04 nm after 5% Fe doping, whereas the microstrain increases from 5.12×10^{-3} to 6.62×10^{-3}. Similarly, the dislocation density increases from 4.62×10^{-2} nm^{-2} to 6.30×10^{-2} nm^{-2}, indicating an increase in lattice imperfections following Fe incorporation. The lattice parameters also decrease, with the *a*-parameter changing from 5.7624 Å to 5.7492 Å and the *c*-parameter from 9.4522 Å to 9.2247 Å, leading to a reduction in the unit-cell volume from 313.87 $Å^3$ to 304.91 $Å^3$. In addition, the calculated bond length decreases from 3.5341 Å to 3.5006 Å, accompanied by a reduction in the distortion parameter. These changes indicate that Fe doping modifies the crystal lattice of Mn_3O_4 and influences its structural characteristics. The observed reduction in volume and shift in the distortion parameter suggest that Fe^{3+} doping effectively modulates the tetragonal symmetry, potentially stabilizing the spinel structure against microstrain [25].

The reduction in the optical band gap from 2.61 eV to 2.38 eV suggests a significant modification of the Mn_3O_4 electronic structure resulting from Fe incorporation. This finding aligns with the structural variations identified via XRD, where Fe doping induces a decrease in crystallite size alongside an increase in microstrain and dislocation density [23,26]. Furthermore, the observed unit cell contraction—caused by the substitution of larger cations with smaller ions—likely disturbs the electronic states near the band edges [24]. Consequently, this narrowed band gap reduces the energy threshold for optical transitions and facilitates enhanced visible-light absorption [27]. Such characteristics render the material advantageous for applications requiring efficient electronic transport and surface-mediated interactions [28]. The function of Fe doping in the creation of defect states that facilitate carrier transitions is underscored by the band gap narrowing, dislocation density, and lattice strain increases. This phenomenon is consistently observed in similar metal oxide thin film systems. In particular, the optical band gap is effectively narrowed by the introduction of dopant-induced sub-bands within the forbidden gap, which enables lower-energy electronic transitions. [12,14].

The enhancement of the surface morphology aligns with the structural parameters derived from XRD. The mean crystallite dimension decreases from 22.14 nm for unadulterated Mn_3O_4 to 20.04 nm after Fe doping, alongside a rise in microstrain and dislocation density. These modifications suggest that the incorporation of Fe affects crystal development during film formation, resulting in a more refined microstructure. The enhancement of these structural characteristics also aids in the observed porous landscape, thereby increasing the effective surface area accessible for surface-dependent activities[29] [30]. This morphological alteration, marked by enhanced porosity and grain refinement, facilitates the enhancement of charge transport kinetics and the electrochemical efficacy of the produced thin films [2].The increased density of grain boundaries in the Fe-doped film modifies the surface area available to the external environment. Charge transport and surface adsorption processes are influenced by particle boundaries in semiconducting metal oxides. The enhanced sensing properties of the Fe-doped Mn_3O_4 thin film are substantiated by the structural alterations observed from XRD, in addition to the morphological transformation.

V. CONCLUSION

The study achieved the successful deposition of pure and 5% Fe-doped Mn_3O_4 thin films thru the spray pyrolysis approach, with comprehensive analyzes uncovering the impact of iron doping on the material's structural, morphological, and optical attributes. The structural optimization and band gap reduction, combined with the observed increase in surface porosity, illustrate that iron doping is a viable method for modifying the physical attributes of Mn_3O_4 thin films. [31]. These findings suggest that Fe-doped Mn_3O_4 thin films are highly promising candidates for advanced optoelectronic and gas-sensing applications where enhanced surface-to-volume ratios and narrow energy band gaps are required [32]. Furthermore, the systematic correlation between structural disorder and optical performance establishes a robust framework for optimizing thin-film growth parameters in future functional device fabrication [33].

ACKNOWLEDGEMENT

The corresponding author acknowledges the financial support from the Chhatrapati Shahu Maharaj Research, Training, and Human Development Organization (SARTHI), Pune, through the Chhatrapati Shahu Maharaj National Research Fellowship (CSMNRF). The author also thanks the Department of Physics for access to the spray pyrolysis facility and the UV-visible spectrophotometer used in this work.

REFERENCES

[1]. Biradar P, Nade A, Dukare S, Chaudhari V. Optimized Spray Pyrolysis Route for Mn_3O_4 Thin Film Synthesis. International Journal of Research Publication and Reviews 2025;6:1856–9. https://doi.org/10.55248/gengpi.6.1025.3618 .
[2]. Augustyn V, Simon P, Dunn B. Pseudocapacitive oxide materials for high-rate electrochemical energy storage. Energy & Environmental Science 2014;7:1597–1597. https://doi.org/10.1039/c3ee44164d .
[3]. Bigiani L, Maccato C, Carraro G, Gasparotto A, Sada C, Comini E, et al. Tailoring Vapor-Phase Fabrication of Mn3O4 Nanosystems: From Synthesis to Gas-Sensing Applications. ACS Applied Nano Materials 2018. https://doi.org/10.1021/acsanm.8b00584 .
[4]. Biradar P, Chaudhari VA. Influence of Cobalt Incorporation on the Structural Evolution and Optical Band Gap of Spray-Pyrolyzed Mn_3O_4 Thin Films. International Journal of Innovative Science and Research Technology (IJISRT) 2026:1581–1581. https://doi.org/10.38124/ijisrt/26jul1094 .
[5]. Rossi Z, Ghannam H, Brioual B, Ullah S, Zanouni M, Diani M, et al. Effect of Cobalt Doping on The Structural, Linear and Nonlinear Optical Parameters of Manganese Oxide Thin Layers. Crystal Research and Technology 2024. https://doi.org/10.1002/crat.202300235 .
[6]. Vignesh R, Sivakumar R, Sanjeeviraja C. A detailed analysis on optical parameters of spinel structured Mn3O4 thin films deposited by nebulized spray pyrolysis technique. Optical Materials 2021. https://doi.org/10.1016/j.optmat.2020.110580 .
[7]. Shano AM, Habeeb AA, Khodair ZT, Adnan SK. Effects of Thickness on the Structural and Optical Properties of Mn3O4 Nanostructure Thin Films. Journal of Physics: Conference Series, 2021. https://doi.org/10.1088/1742-6596/1818/1/012049
[8]. He L, Zhang G, Dong Y, Zhang Z, Xue S, Jiang X. Polyetheramide Templated Synthesis of Monodisperse Mn3O4 Nanoparticles with Controlled Size and Study of the Electrochemical Properties. Nano-Micro Letters 2014;6:38–45. https://doi.org/10.1007/bf03353767 .
[9]. Dahamni MA, Ghamnia M, Naceri SE, Fauquet C, Tonneau D, Pireaux J, et al. Spray Pyrolysis Synthesis of Pure and Mg-Doped Manganese Oxide Thin Films. Coatings 2021;11:598–598. https://doi.org/10.3390/coatings11050598 .
[10]. Paudel TR, Zakutayev A, Lany S, d'Avezac M, Zunger A. Doping Rules and Doping Prototypes in A2BO4 Spinel Oxides. Advanced Functional Materials 2011;21:4493–501. https://doi.org/10.1002/adfm.201101469 .
[11]. Belkhedkar MR, Ubale AU. Physical properties of Fe doped Mn 3 O 4 thin films synthesized by SILAR method and their antibacterial performance against E. coli. Journal of Saudi Chemical Society 2014;20:553–60. https://doi.org/10.1016/j.jscs.2014.11.004 .
[12]. Zhang S, Li H, Wu Z, Post JE, Lanson B, Elzinga EJ, et al. Effects of Co doping on the structure and physicochemical properties of hausmannite (Mn3O4) and its transformation during aging. Chemical Geology 2021;582:120448–120448. https://doi.org/10.1016/j.chemgeo.2021.120448 .
[13]. Tholkappiyan R, Naveen AN, Vishista K, Hamed F. Investigation on the electrochemical performance of hausmannite Mn3O4 nanoparticles by ultrasonic irradiation assisted co-precipitation method for supercapacitor electrodes. Journal of Taibah University for Science 2018;12:669–77. https://doi.org/10.1080/16583655.2018.1497440 .
[14]. Diallo A, Tandjigora N, Ndiaye S, Jan T, Ahmad I, Mâaza M. Green synthesis of single phase hausmannite Mn3O4 nanoparticles via Aspalathus linearis natural extract. SN Applied Sciences 2021;3. https://doi.org/10.1007/s42452-021-04550-3 .
[15]. Nadeem A, Bashir AI, Azam S, Rahman AU, Iqbal MA. On the role of Zn doping on tuning the electronic and optical properties of MnCr 2 O 4 spinel via Mn

ISSN No:-2456-2165 https://doi.org/10.38124/ijisrt/26aug363

0.5 Zn 0.5 Cr 2 O 4 doping scheme: A first-principles quantum computational analysis. Physica Scripta 2022;97:45812–45812. https://doi.org/10.1088/1402-4896/ac5bbf .

[16]. Vignesh R, Sivakumar R, Sanjeeviraja C. Phase tuning of nebulized spray deposited manganese oxide thin films by the effect of annealing temperature and their linear and non-linear optical parameters - ScienceDirect n.d.:168687–168687. https://doi.org/10.1016/j.ijleo.2022.168687 .

[17]. Karpagavalli S, Vethanathan SJK, Perumal S. Spectroscopic and Superparamagnetic Behaviour of Hausmannite Manganese Oxide Nanoparticles. Asian Journal of Chemistry 2019;31:793–8. https://doi.org/10.14233/ajchem.2019.21729 .

[18]. Najim AA, Gbashi KR, Salih AT. Synthesis and Characterization of Nanocrystalline Ba-doped Mn3O4 Hausmannite Thin Films for Optoelectronic Applications. International Journal of Nanoscience 2021;20. https://doi.org/10.1142/s0219581x2150040x .

[19]. Sukhdev A, Challa M, Narayani L, Manjunatha AS, Deepthi PR, Angadi VJ, et al. Synthesis, phase transformation, and morphology of hausmannite Mn3O4 nanoparticles: photocatalytic and antibacterial investigations. Heliyon 2020;6. https://doi.org/10.1016/j.heliyon.2020.e03245 .

[20]. Tian Z, Kouotou PM, Bahlawane N, Ngamou PHT. Synthesis of the Catalytically Active Mn3O4 Spinel and Its Thermal Properties. The Journal of Physical Chemistry C 2013;117:6218–24. https://doi.org/10.1021/jp312444s .

[21]. Baykal A, Kavas H, Durmuş Z, Demir M, Kazan S, Topkaya R, et al. Sonochemical synthesis and chracterization of Mn3O4 nanoparticles. Open Chemistry 2010;8:633–8. https://doi.org/10.2478/s11532-010-0037-8 .

[22]. Xia S, Yu Z, Wei Z, Liu L. Mechanistic Investigation of Enhancing ZnO Gas-Sensing Performance through Manganese Doping and Heterostructure Construction: A Combined Theoretical and Experimental Approach. Langmuir 2025;41:21925–35. https://doi.org/10.1021/acs.langmuir.5c00793 .

[23]. Tonu NT, Ahamed P, Yousuf M. Rice powder template for hausmannite Mn3O4 nanoparticles and its application to aqueous zinc ion battery. PLoS ONE 2024;19. https://doi.org/10.1371/journal.pone.0305611 .

[24]. Dubal DP, Dhawale DS, Salunkhe RR, Pawar SM, Fulari VJ, Lokhande CD. A novel chemical synthesis of interlocked cubes of hausmannite Mn3O4 thin films for supercapacitor application. Journal of Alloys and Compounds 2009. https://doi.org/10.1016/j.jallcom.2009.03.135 .

[25]. Venkatesh R, Ravidhas C, Sivakumar R, Dhandayuthapani T, Pitchaimuthu S, Sanjeeviraja C, et al. Analysis of optical dispersion parameters and electrochromic properties of manganese-doped Co3O4 dendrite structured thin films. Journal of Physics and Chemistry of Solids 2018;122:118–29. https://doi.org/10.1016/j.jpcs.2018.06.015 .

[26]. Zhou T, Liu X, Zhang R, Wang L, Zhang T. Constructing Hierarchical Heterostructured Mn3O4/Zn2SnO4 Materials for Efficient Gas Sensing Reaction. Advanced Materials Interfaces 2018;5. https://doi.org/10.1002/admi.201800115 .

[27]. Doubi Y, Hartiti B, Siadat M, Labrim H, Fadili S, Tahri M, et al. Experimental Investigation of Pure Spinel Mn3O4 Properties Synthesized through Chemical Spray Pyrolysis for Future Gas Sensor Application. European Journal of Inorganic Chemistry 2023;26. https://doi.org/10.1002/ejic.202300047 .

[28]. Bigiani L, Maccato C, Gasparotto A, Sada C, Barreca D. Structure and properties of Mn3O4 thin films grown on single crystal substrates by chemical vapor deposition. Research Padua Archive (University of Padua) 2018;223:591–6. https://doi.org/10.1016/j.matchemphys.2018.11.047 .

[29]. Saruhan B, Fomekong RL, Nahirniak S. Review: Influences of Semiconductor Metal Oxide Properties on Gas Sensing Characteristics. Frontiers in Sensors 2021;2. https://doi.org/10.3389/fsens.2021.657931 .

[30]. Sun Y, Liu S, Meng F, Liu J, Jin Z, Kong L, et al. Metal Oxide Nanostructures and Their Gas Sensing Properties: A Review. Sensors 2012;12:2610–31. https://doi.org/10.3390/s120302610 .

[31]. Jabir NA, Rasheed HS, Jassim RI. Physical Properties of Zinc Doping on the Nanostructured Fe_2O_3 Thin Films Deposited by Chemical Spray Pyrolysis Technique. International Journal of Scientific Research in Science Engineering and Technology 2025;12:508–16. https://doi.org/10.32628/ijsrset2512535 .

[32]. Patil TS, Kothavale VP, Malekar VP, Kamble RS, Patil RB, Gurav KV, et al. Effect of Nickel (Ni) Ion Doping on the Morphology and Supercapacitive Performance of Mn3O4 Thin Films. Journal of Electronic Materials 2024. https://doi.org/10.1007/s11664-023-10765-4 .

[33]. Gore D, Phulmante A, Londhe C. Systematic Approach to Higher Fe Doping in CuO Materials. International Journal of Innovative Science and Research Technology (IJISRT) 2026:1338–1338. https://doi.org/10.38124/ijisrt/26mar793 .